CIRP Annals - Manufacturing Technology xxx (2018) xxx–xxx

Contents lists available at ScienceDirect

CIRP Annals - Manufacturing Technology

journal homepage: http://ees.elsevier.com/cirp/default.asp

Basic principles for the design of cutting edge roundings

Benjamin Bergmann *, Thilo Grove

Institute of Production Engineering and Machine Tools IFW, Leibniz Universität Hannover, Germany

Submitted by K. Weinert (1), Dortmund, Germany

ARTICLE INFO

Keywords:
Cutting edge
Design
Modelling

ABSTRACT

Adapted cutting edge roundings lead to a performance increase of cutting tools. The optimal cutting edge design is determined by the thermomechanical process load and thus depends on the machined material. In this study, the external mechanical load is investigated in direct relation to material properties by means of microcinematography. It could be shown that load characteristics are mainly material independent, whereas the load level depends on the machined material. Finally, the findings were transferred into a model, which enables the design of cutting edge roundings based on material properties.

1. Introduction

The cutting edge shape is of decisive importance for the performance of the tool in cutting applications. The increased performance of appropriately shaped cutting edges is attributed to reduced stresses in the wedge due to higher stability and an increased contact section between tool and workpiece. However, there is no existing model that allows for material-based design of cutting edge microgeometries. This is due to the fact that the necessary knowledge for the design of the cutting edge rounding, such as load stresses have not been adequately studied and thus are not sufficiently known. The determination of local mechanical stresses in the wedge of cutting tools is still one of the major challenges in machining [1]. The distribution of stress influences tool failure and thus its productivity. In order to determine the stress distribution in the wedge, various experimental [2] and theoretical studies [3] are available. An overview is also given in Ref. [3]. It can be stated that the stress distribution in the wedge cannot be determined with sufficient accuracy neither with experimental nor finite element chip formation simulation. Especially the different boundary conditions of the finite element simulation, e.g. material and friction models, have a significant influence on the simulation result [4]. In particular, no findings regarding the stress distribution based on experimental data exist with respect to the cutting edge rounding. For these reasons, in this work an understanding of the formation of load stresses in the cutting wedge in relation to the cutting edge microgeometry and the material properties is investigated.

2. Experimental setup

The experiments regarding the stress distributions in the cutting edge were conducted on a planing test rig in two steps [5]. First, geometric contact conditions were determined. Secondly, the chip formation was investigated in detail. The linear direct drive of the planing test rig is capable of a maximum cutting speed of v_c = 180 m/min. During the experiments, the process forces were measured with a Kistler type 9257B dynamometer. The chip formation was analysed with a high speed camera Photron Fastcam Type SA5 and a mounted lens by Navitar. In order to avoid motion blur and to ensure sufficient brightness, a xenon cold light by Storz type Techno light 270 was used. For the contact length measurement, 16,000 frames per second were chosen to guarantee a sufficient field of view. Detailed analyses in the shear zone were conducted with 40,000 frames per second, narrowing down the field of view to 320 × 256 pixels. Process forces and high speed imaging were synchronized by using a trigger signal from the high speed camera. To ensure plain strain conditions during machining, workpiece and tool were mounted against sapphire glass. In the contact zone between tool and glass, immersion oil was applied to achieve the best optical conditions. The width of the undeformed chip was set to b = 3 mm and a cutting speed of v_c = 120 m/min was used. The undeformed chip thickness was altered continuously from h = 0 mm up to a constant undeformed chip thickness value of $h_{,const}$ = 0.1 mm. This enabled the analysis of the influence of increasing undeformed chip thickness on process forces, chip formation, and contact length within a single experiment. The cutting length with variation of h was set to l_c = 100 mm, while the constant part presented a cutting length of l_c = 20 mm. Experimental wear investigations were carried out on the CTX520 linear without coolant during orthogonal turning with v_c = 120 m/min and f = h = 0.1 mm. The width of the undeformed chip was identical to that of the planing investigations. The used material and their properties in this study are summarized in Table 1.

For the cutting tests, macrogeometry and microgeometry identical to Ref. [6] were chosen. Coated cemented carbide (82.0 wt% WC, 10 wt % Co and 8 wt% MC) inserts (SNMA190612) with a PVD-nanolayer of TiN–TiAlN were used. All applied cutting tools were produced in one batch. In order to mount the tool onto the glass and to avoid material

* Corresponding author.
E-mail address: bergmann@ifw.uni-hannover.de (B. Bergmann).

https://doi.org/10.1016/j.cirp.2018.04.019
0007-8506/© 2018 Published by Elsevier Ltd on behalf of CIRP.

Nomenclature

Formula directory

b	Width of undeformed chip
cl	Contact length
cl_α	Contact length (section I)
$dF_{N\gamma}$	Incremental normal force on the rake face
$dF_{T\gamma}$	Incremental tangential force on the rake face
$F_{c\alpha,\delta}$	Proportional process force in cutting direction (section I)
$F_{c,hmin}$	Cutting force at the minimum chip thickness
$F_{c\varepsilon}$	Cutting force in section II
$F_{f,hmin}$	Feed force at the minimum chip thickness
$F_{f\alpha;\varepsilon;\gamma}$	Feed force in section I; section II; section III
$F_{f\alpha,\delta}$	Proportional process force in feed direction (section I)
F_N	Normal force
$F_{N\alpha;\varepsilon;\gamma}$	Normal force in section I; section II; section III
F_T	Tangential force
$F_{T\alpha;\varepsilon;\gamma}$	Tangential force in section I; section II; section III
h_{el}	Elastic chip thickness springback
h_{min}	Minimum chip thickness
n_γ	Stress distribution index (section III)
Δl	Arc length in each stress increment (section III)
l_{cl}	Effective arc length depending on the contact length
l_h	Effective arc length depending on the undeformed chip thickness
l_ε	Arc length of the cutting edge between point 0 and h_{min}
γ_{eff}	Effective rake angle
ε_f	Material springback
η	Tangential stress factor
$\eta_{\varepsilon f}$	Material springback ratio
η_{hel}	Relative springback ratio
λ	Chip compression ratio
μ_{av}	Average coefficient of friction (section III)
μ_ε	Stress ratio in section II
$\sigma_{\alpha;\varepsilon;\gamma}$	Normal stress in section I; section II; section III
$\tau_{\alpha;\varepsilon;\gamma}$	Tangential stress in section I; section II; section III
Φ	Shear angle

flow between both, the corner radius was removed by grinding. Given the tool holder, a rake angle of $\gamma = -6°$ was set. The cutting edge preparation was done by means of brushing. For all cutting edge radii, the standard deviation is 10% related to the nominal target of the cutting edge radius. The characterization of the rounded cutting edges is based on Denkena et al. [7], extended by the method of Bassett et al. [6]. They introduced the effective length of the cutting edge radius (l_α and l_γ) with l_α describing the arc length of the cutting radius on the flank face and l_γ on the rake face respectively.

Table 1
Mechanical properties of the investigated materials.

Material	Tensile strength R_m [MPa]	Yield strength $R_{p0.2\%}$ [MPa]	Young's modulus E [GPa]
70MnVS4	888	507	210
AISI 1045 (hardened)	770	475	210
AISI 1045	608	310	210
AISI 1045 (annealed)	539	250	210
Ti6Al4V	947	880	114
EN AW-7075	558	501	71.7
EN AW-2007	365	205	73

3. Mechanical load on the cutting edge

In cutting, minimum chip thickness h_{min}, contact length cl, and elastic chip thickness springback h_{el} determine the loaded surfaces on the cutting tool, as displayed in Fig. 1. If, additionally, the process forces are known, the calculation of load stresses is possible. The sections are derived from the phases of chip formation. Each phase is characterized by distinct differences in material deformation and thus differing load conditions. In the first phase, chip formation is characterized by elasto-plastic material deformation; sections I and II are loaded. Section I ranges from the lowest point on the cutting wedge (point 0) to the end of the material contact on the flank face due to elastic material springback (point A). Section II is located between point 0 and the contact point of the minimum chip thickness. When initiating chip formation, sections I and II are progressively loaded with increasing chip thickness due to the simultaneous gain of contact with the material. Once h_{min} is surpassed, chip formation begins, the shear zone forms, and section III is loaded.

This section ranges from the point of contact at h_{min} up to the point of chip separation and thus defines the contact length cl. Below, the determination of mechanical stresses will be presented for each of the three sections based on the results of Ref. [5] by means of a combination of process force and contact section measurements with analytical and simulative investigations. The approach is the same for each section:

(a) Determination of process forces in the coordinates system of the workpiece.
(b) Determination of the contact length.
(c) Transformation of process forces into tool coordinates.
(d) Definition of an approach for the stress distribution.
(e) Determination of the stress distribution.

3.1. Section I

(a) A workpiece tool contact in section I requires contact in section II and thus hinders the exclusive analysis of contact length and process forces in each of these two sections. Therefore, the experimental method of setting back the flank face by means of laser ablation was used. The application of laser material processing for the high-precision preparation has been demonstrated in Ref. [8]. With this method, the analysis can be carried out for section II (having set back the flank face) and for section I.

By subtracting the measured process forces without a flank face from those with one, the proportional process forces in section I and II can be determined locally. The necessary experimental machining tests were carried out in orthogonal turning at $v_c = 300$ m/min to avoid cutting edge failure, which occurred using a cutting speed of $v_c = 120$ m/min. First, the proportional process forces at the flank face in cutting direction, $F_{c\alpha,\delta}$, and in feed direction, $F_{f\alpha,\delta}$, were determined for AISI 1045. They are shown as a function of the minimum chip thickness in Fig. 2.

For the minimum chip thickness, the values of Bassett were used [9]. It was found that with increasing minimum chip thickness and thus elastic chip thickness springback, the process forces on the flank face increase. The proportional feed forces at flank face increase by factor 2.8 from 5% to 14% with an increment in the minimum cutting thickness due to the cutting edge rounding

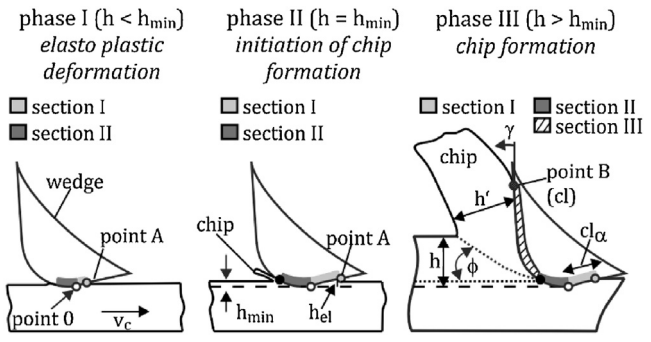

Fig. 1. Phases of chip formation and resulting contact sections.

Please cite this article in press as: Bergmann B, Grove T. Basic principles for the design of cutting edge roundings. CIRP Annals - Manufacturing Technology (2018), https://doi.org/10.1016/j.cirp.2018.04.019